Assessing the Risk of Internal Erosion in Embankments and Foundations

Ishant Sharma[1] and Ashish Juneja[2]

[1] UG Student, Department of Civil Engineering, Punjab Engineering College, Chandigarh
[2] Professor, Department of Civil Engineering, Indian Institute of Technology Bombay, Mumbai
Ishantsharma.becivil16@pec.edu.in

Abstract Internal erosion by piping is one of the main causes responsible for the failure of earth structures such as embankments, dams and foundations. This phenomenon occurs when concentrated leakage develop in pre-existing defects in the soil structures. The erosion characteristics are described by the erosion rate index ranging from 0 to 6 indicating that the rate of erosion of soil can vary up to 10^6 times.

To study this complex behavior, a new experimental device was developed to simulate the conditions of internal erosion. It was designed using CAD and made-up of stainless steel. It mainly consisted of a semi cylindrical mold and rectangular sheet made of perspex. A digital camera was used to capture the propagation of groove in the soil to measure the internal erosion characteristics.

The effect of plasticity index and fine fraction on the rate of internal erosion and critical shear stress were studied. A series of erosion tests were performed under constant head loss in order to quantify the critical shear stress (τ_c) and the coefficient of piping erosion (k_{er}) of five different soils. It was observed that critical shear stress increased while coefficient of soil erosion decreased with increase in fine fraction. An easy, quick and economical approach which could be applicable in both constructed earth structures and natural river banks for determining their susceptibility to internal erosion was achieved through this study.

Keywords: Coefficient of Piping; Critical Shear Stress; Erosion Rate Index; Internal erosion, Plasticity index

1 Introduction

Study of dam failures has been one of the most prevailing topics in geotechnical engineering. This phenomenon primarily occurs due to overtopping, slope instability, earthquake and internal erosion. The latter being the most complex and less understood one. In this specific research area, several researchers focus on two soil erosion parameters: critical shear stress and erosion rate per unit surface area. Different researchers developed different devices to calculate the erodibility of the soil. Flume tests (Gibbs 1962; Kandiah and Arulanandan 1974; Arulanandan and Perry 1983), jet erosion test (Moore and Masch 1962; Hanson 1991; Hanson and Robinson 1993), rotating cylinder test (Moore and Masch 1962; Sargunan 1977; Chapuis and Gatien 1986) and erosion test apparatus by (Briaud et al. 2001) are few critical developments among many in determination of soil erosion characteristics.

However, the relationship between the erosion parameters, geotechnical and physicochemical properties of soils still remain in the nascent stage of research. This study hence focuses on determination of these parameters through development of a device based on energy equations and theory of fluid mechanics.

2 Theory

As mentioned in the earlier section erodibility characteristics of soil can be determined from critical shear stress and erosion rate index. Where, the former is the stress at which significant amount of soil particle suddenly detaches itself from the parent structure and the latter is the measure of rate of erosion.

Relationship between the rate of erosion and the applied hydraulic shear stress can be expressed as

$$\varepsilon_t = c_e(\tau_t - \tau_c) \tag{1}$$

where ε_t is the rate of erosion per unit surface area of the slot/hole at time t (kg/s/m^2), c_e is the proportionality constant or commonly known as the coefficient of soil erosion (s/m), τ_t is the hydraulic shear stress along the slot/hole at time t (N/m^2), τ_c is the critical shear stress (N/m^2).The value of c_e varies from 10^{-1} to 10^{-6} (s/m). The -log (c_e) is used in correlation analysis and plotting the results. The erosion rate index (I), defined as I= -$log(c_e)$ ranging from 0 to 6. A lower value of I implies a more rapidly erodible soil. The critical shear stress τ_c can be obtained by using the increasing portion of the curve and linearly extrapolating the best fit to zero, when ε_t is plotted against τ_t as done in (Wan and Fell 2002, 2004a, 2004b). However, this can be better defined by successive HETs with different heads.

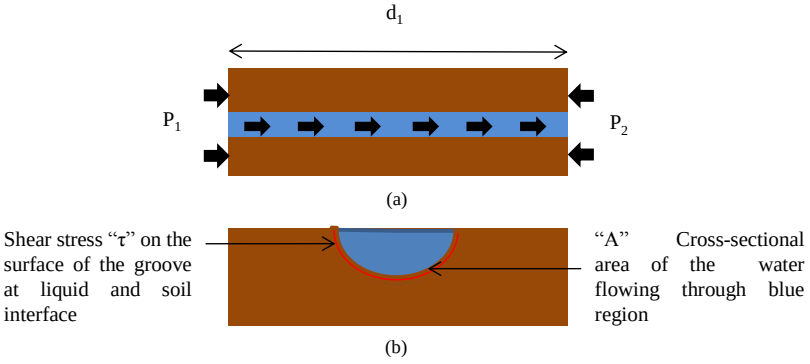

Figs. 1 (a) Top view, (b) front view of soil sample.

Applying the force equilibrium equation between flowing fluid and soil groove as shown in the following equation

$$\boldsymbol{\tau . P . d_l = A . d_p} \tag{2}$$

where τ is the hydraulic shear stress along the wetted area of the groove, *"P"* is the wetted parameter of semicircular groove which was equal to ($\pi\phi/2$), d_l is the small length of the groove along the direction of flow is the diameter of groove, "*A*" is area of cross-Section of the groove which is equal to ($\pi\phi^2/8$) and d_p is the hydraulic pressure loss during the flow.

Figure 1 shows the working principle of the device where P_1, P_2 represents the pressures at the inlet and outlet end respectively. Where P_1-P_2 is equal to the head loss d_p along the length d_1 Pressure head loss d_p can be expressed in the form of dh_f friction head loss as shown below.

$$d_p = \rho . g . dh_f \tag{3}$$

Substituting the values of *P* and *A* in Eq (2) we get,

$$\tau . \frac{\pi.\phi}{2} = \frac{\pi.\phi^2}{8} . \frac{\rho.\mathrm{g}.dh_f}{d_l} \tag{4}$$

Solving Eq (4) further we get,

$$\tau = \frac{\phi}{4} . \frac{\rho.\mathrm{g}.dh_f}{d_l} \tag{5}$$

where (dh_f/d_l) in Eq (5) is known as friction head loss gradient.

Few assumptions made in the above derivation are as follows:

1. Flow through the soil matrix was taken negligible;

2. Only the soil surface along the preformed hole provided shear resistance;

3. Diameter of the semicircular groove was averaged throughout the length of the soil specimen;

4. Hydraulic head difference across the soil specimen, d_p equals total friction head loss h_f.

Further, Erosion rate per unit surface area is given by

$$\varepsilon_t = \frac{\rho_d}{P.L} . \frac{d(A.L)}{dt} \quad (6)$$

where ρ_d in the above is the dry density of the compacted soil sample and *d(A.L)/dt* is the rate of change in the volume of compacted soil with the flow of water.

Differentiating *(A.L)* with respect to time we obtain

$$d(A.L) = L.d(A) + A.d(L) \quad (7)$$

As length is assumed to be constant with respect to time, *d(L)* is 0.
Substituting the value of *P*, *A* and Eq (6) in Eq (5) we get

$$\varepsilon_t = \rho_d . [L.d\left(\frac{\pi.\phi^2}{8}\right) + A.0] / (dt . \frac{\pi.\phi.L}{2}) \quad (8)$$

Rate of change of cross-sectional area of the groove is:

$$\frac{d(\pi.\phi^2)}{8.d(t)} = \frac{\pi.\phi}{4} . \frac{d(\phi)}{d(t)} \quad (9)$$

By using Eq (8), Eq (7) was modified to

$$\varepsilon_t = \rho_d . (\frac{\pi.\phi.d(\phi).L}{4.d(t)}) / \left(\frac{\pi.\phi.L}{2}\right) \quad (10)$$

Solving Eq (10) we get,

$$\varepsilon_t = \frac{\rho_d}{2} . \frac{d(\phi)}{d(t)} \quad (11)$$

As proved and shown in Eq (10) that erosional rate per unit surface area of the groove depends only on dry density at which the soil is compacted and rate of change of diameter of the groove. Following Assumptions were made during its derivation

1. Length of groove assumed to be constant throughout.
2. Erosion in the grove was uniform throughout the perimeter

3 Experimental Set up

The effect of crack development in dams and embankments had been simulated by developing the groove erosion device. Tests were performed on five different soil samples having different fine fractions. Data obtained was used to calculate the erosional characteristics of soil.

Description of erosion test apparatus

A new experimental device was developed to simulate the condition of the internal erosion. The device mainly consists of three parts.

- Inlet end
- Main module
- Outlet end

As shown in Figure 2 (a,b,c) inlet end was connected to the inlet coupling where constant inlet head was maintained throughout the test. Main module consists of two sub-parts: i) semi cylindrical perspex of internal diameter 34mm and thickness 2 mm in order to hold the grooved soil sample. ii) top perspex of 7.5 mm thickness to visualize the rate of change of diameter of the grove. Porous stones were placed on the either end of the main module and were prepared using 75μ passing sand and adhesive. Outlet end was connected to the T-valve, one end of it was connected to the piezometer and the other was connected to the filter tank.

Figure 3 shows the complete experimental set up where red colored water was stored in the constant head device. Groove erosion apparatus and camera stand was fixed on the base plate to avoid relative motion between them. One end of Outlet T-valve was connected to filtering tank and other was connected to stand pipe. Water collected in the tank was used in the subsequent tests.

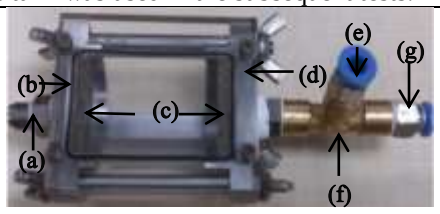

(a)

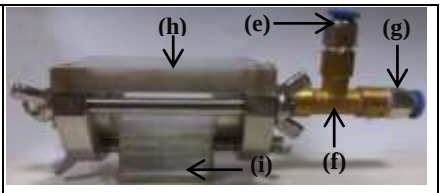

(b)

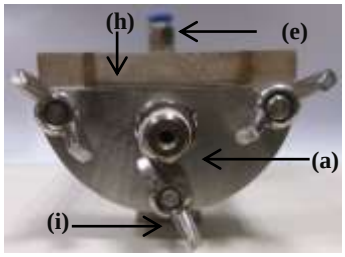

(c)

(a) Inlet coupling
(b) Inlet end
(c) Porous stone
(d) Outlet end
(e) Piezometer connection
(f) T-valve
(g) Discharge outlet
(h) Top Perspex
(i) Stand

Figs. 2(a-c) (a) top view, (b) side view (c) front view of the groove erosion test apparatus

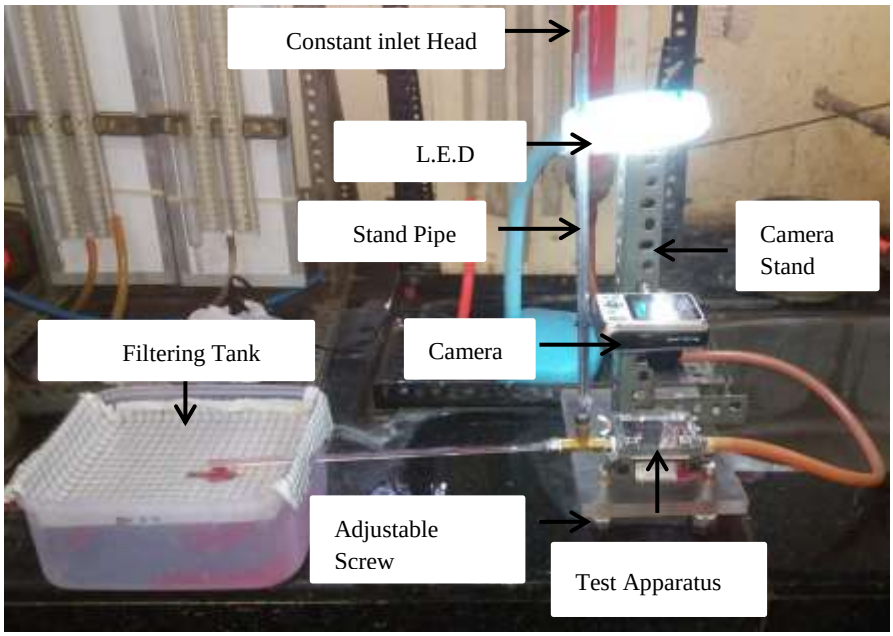

Fig. 3 Groove Erosion Test Setup

3.1 Material used

It is essential to study the percentage of fines in different soils for understanding each's erosional properties. For the current research the properties of different soils are given in Table 1.

Table 1 Material Properties

Type of soil	Fine Fraction (%)	P.L (%)	L.L (%)	P.I (%)
Black cotton soil	80	30.12	74.66	44.54
Black dust	20	34.11	68	33.89
Powai silt	50	22.25	31.7	9.45
Marine clay	82	35.21	72.39	37.18
Kaolin	94	38.31	78.41	41.1

3.2 Experimental Procedure

Soil samples were compacted inside the cylindrical mold at optimum moisture content and maximum dry density. The samples are then extracted using extruder trimmed and placed inside the semi cylindrical perspex. Further, the 6mm grove was made using Sharpe needle. Sample was then placed inside the mold and closed using perspex. A constant inlet head was maintained by performing few initial trials till considerable erosion was initiated for a given soil. Test was then continued till thirty minutes. Outlet head was measured and continuous pictures were taken at regular interval of five minutes using camera. Red dye was mixed with the water to distinguish the change of diameter within the subsequent images. Change of diameter was measured using camera measure software.

4 Results and Discussions

Five different soil samples were taken black cotton and black dust from railway's embankment in Sholapur, Powai silt from the littoral zone of Powai lake, kaolin from Nagpur and marine clay from shores of Maharashtra. These soils have different percentages of fine fraction. All the samples were compacted at a moisture content and dry density according to the guidelines provided by Standard proctor test procedure (IS-2720-PART-7-1980). Tap water was used as an eroding fluid and all the tests were conducted on these compacted samples.

4.1 Effect of percentage fine fraction on I-value

Figure 4 shows effect of different fine fraction percentage on *I* value obtained from a typical experiment of a groove erosion test carried out on five different soil samples. It was observed that with the increase in the percentage of fine fraction erosion rate decreased and *I* value increased. Lesser values of *I* indicate rapid erosion. A better correlation could not be established between them due to the effect of soil mineralogy and corresponding plasticity index.

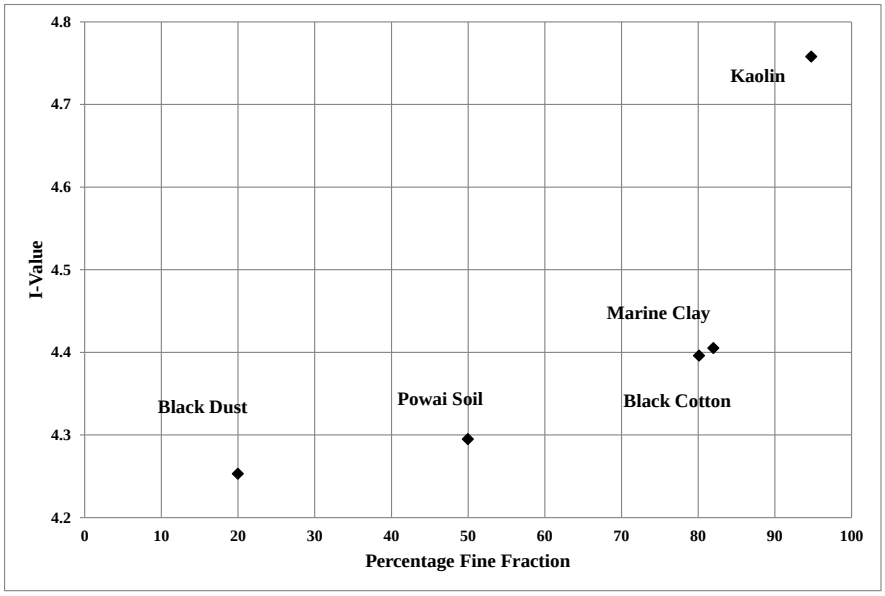

Fig.4 Relation between *I*-value and Percentage Finer

4.2 Effect of percentage fine fraction on critical shear stress

The soil samples consisting of different fractions of fines were tested to evaluate the effect of critical shear stress on the amount of fine fraction present in a given soil. Fig 5 shows as the fine content increased the soil grains were more tightly packed which resulted in a stronger interlocking among the grains which further resulted in the higher value of critical shear stress.

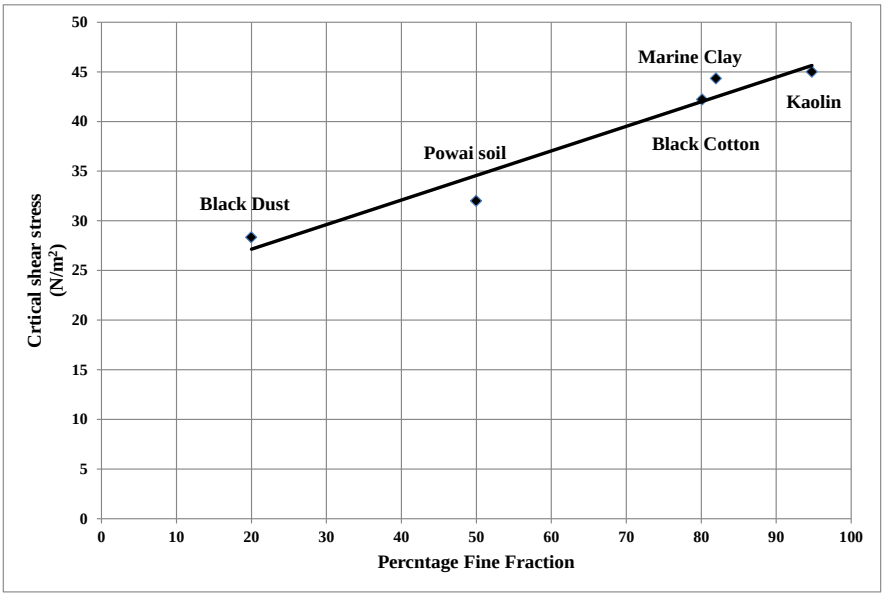

Fig.5 Relation between Critical Shear stress and Percentage Finer

4.3 Characterization of erosional behavior of soil on the basis of plasticity index

Figure 6 shows the characterization of five soil samples for different plasticity index. The tests conducted were used to understand the effect of plasticity index and percentages of fines on critical shear stress. As plasticity index increases soil tend to shift towards the higher ranges of critical shear stress. The reason for this behavior is the increase in cohesion with progressive increase in plasticity index of soil. The fine fraction present in soil also imposes the limits on critical shear stress value. Higher fine fraction results in good interlocking of soil grains which results in higher values of critical shear stress. However, with passage of time the rate of erosion in the groove first decreases and then increases. The first decreasing trend is due to the lesser increase in groove diameter and with increase in time soil near the groove gets saturated and the cohesion value decreases which results in loosening of the soil grains thereby increasing erosion rate.

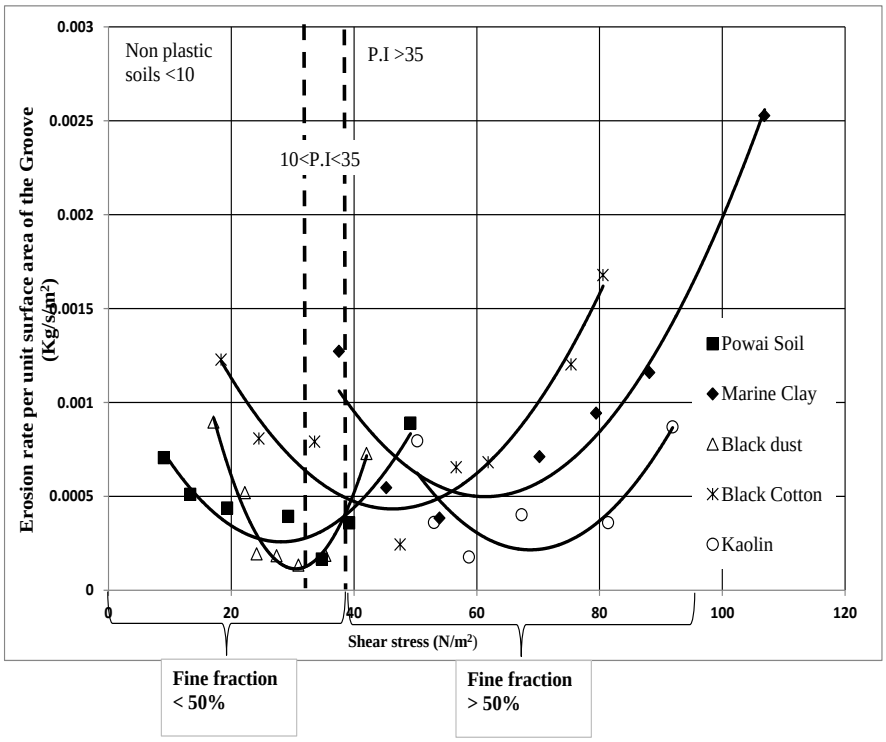

Fig.6 Characterization of erosional behavior of soil on the basis of plasticity index

5 Conclusions

The critical shear stress for erosion of the soil increased with increase in percentage finer linearly. It was observed that critical shear stress increased by 9 % with 50 % increase in fine fraction. Erosion rate decreased with increase in fine fraction. On the other hand, a better correlation could not have been produced between them as the soil mineralogy and corresponding plasticity index also played a significant role in the erosion rate. A combined effect of plasticity index and percentage finer was determined in this study. It was found that for plasticity index in between 10% to 35% critical shear stress varied from 32 N/m^2 to 40 N/m^2 for soil having fine fraction less than 50%.As plasticity index increased cohesion between the grains of the soil also increased. Both plasticity index and percentage finer have significant effect on the erosional characteristics of soil. From the experimental set up developed in the current research work it was seen that with increase in the time and as head loss incurred the rate of erosion initially decreases and with progress in time it increases. Minimum erosion rate was observed at the point of saturation and follows a parabolic path.

6 Acknowledgments

The first author would like to thank Industrial Research and Consultancy Center (IRCC) IIT Bombay for the scholarship during the internship programme at IIT Bombay. IRCC also sponsored the testing and equipment used in this study.

7 References

Arulanandan, K., Perry, E. B.: Erosion in relation to filter design criteria in earth dams. Journal of Geotechnical Engineering, 109(5), 682-698, (1983).

Briaud, J. L., Ting, F. C. K., Chen, H. C., Cao, Y., Han, S. W., Kwak, K. W.: Erosion function apparatus for scour rate predictions. Journal of geotechnical and geoenvironmental engineering, 127(2), 105-113, (2001).

Chapuis, R. P., Gatien, T.: An improved rotating cylinder technique for quantitative measurements of the scour resistance of clays. Canadian geotechnical journal,23(1), 83-87, (1986).

Fell, R., Wan, C. F., Cyganiewicz, J., Foster, M.: Time for development of internal erosion and piping in embankment dams. Journal of geotechnical and geoenvironmental engineering, 129(4), 307-314, (2003).

Foster, M., Fell, R.: Assessing embankment dam filters that do not satisfy design criteria. Journal of Geotechnical and Geoenvironmental Engineering, 127(5), 398-407, (2001).

Ghebreiyessus, Y. T., Gantzer, C. J., Alberts, E. E., & Lentz, R. W.: Soil erosion by concentrated flow: shear stress and bulk density. Transactions of the ASAE, 37(6), 1791-1797, (1994).

Hanson, G. J.: Development of a jet index to characterize erosion resistance of soils in earthen spillways. Transactions of the ASAE, 34(5), 2015-2020, (1991).

Hanson, G. J., Robinson, K. M.: The influence of soil moisture and compaction on spillway erosion. Transactions of the ASAE, 36(5), 1349-1352, (1993).

Hjeldness, E. I., Lavania, B. V.: Cracking, leakage, and erosion of earth dam materials. Journal of Geotechnical and Geoenvironmental Engineering, 106(ASCE 15220), (1980).

Maranha, D.N.: Analysis of Crack Erosion in Dam Cores. The Crack Erosion Test. De Mello Volume, 284-298, (1989).

Reddi, L. N., Lee, I. M., Bonala, M. V.: Comparison of internal and surface erosion using flow pump tests on a sand-kaolinite mixture. Geotechnical testing journal, 23(1), 116-122, (2000).

Sanchez, R. L., Strutynsky, A. I., Silver, M. L.: Evaluation of the erosion potential of embankment core materials using the laboratory triaxial erosion test procedure (No. WES/TR/GL-83-4). Army Engineer Waterways Experiment Station Vicksburg Ms Geotechnical Lab, (1983).

Sargunan, A.: Concept of critical shear stress in relation to characterization of dispersive clays. Dispersive Clays, Related Piping, and Erosion in Geotechnical Projects, Symp., 79th Annual Meeting, American Society for Testing and Materials, , ASTM Special Technical Publication 623, Sherard, J. L. and Decker, R. S., eds., 390–397. Chicago , (1977).

Shaikh, A., Ruff, J. F., Abt, S. R.: Erosion rate of compacted Na-montmorillonite soils. Journal of geotechnical engineering, 114(3), 296-305, (1988).

Sherard, J. L., Dunnigan, L. P.: Filters and leakage control in embankment dams. In Seepage and leakage from dams and impoundments (pp. 1-30). ASCE, (1985).

Sherard, J. L., Dunnigan, L. P.: Critical filters for impervious soils. Journal of Geotechnical Engineering, 115(7), 927-947, (1989).

Garg, SK.: Soil mechanics and foundation engineering. 9th edn. Khanna Publishers, New Delhi(2012).